Phagocytosis executes delayed neuronal death after focal brain ischemia

Jonas J. Neher[a,b,1], Julius V. Emmrich[a], Michael Fricker[a,2], Palwinder K. Mander[a,3], Clotilde Théry[c], and Guy C. Brown[a,1]

[a]Department of Biochemistry, University of Cambridge, Cambridge CB2 1QW, United Kingdom; [b]Department of Cellular Neurology, Hertie Institute for Clinical Brain Research, University of Tübingen, 72076 Tübingen, Germany; and [c]Institut Curie, Institut National de la Santé et de la Recherche Médicale U932, 75248 Paris, France

Edited by Ruslan Medzhitov, Yale University School of Medicine, New Haven, CT, and approved September 18, 2013 (received for review May 8, 2013)

Delayed neuronal loss and brain atrophy after cerebral ischemia contribute to stroke and dementia pathology, but the mechanisms are poorly understood. Phagocytic removal of neurons is generally assumed to be beneficial and to occur only after neuronal death. However, we report herein that inhibition of phagocytosis can prevent delayed loss and death of functional neurons after transient brain ischemia. Two phagocytic proteins, Mer receptor tyrosine kinase (MerTK) and Milk fat globule EGF-like factor 8 (MFG-E8), were transiently up-regulated by macrophages/microglia after focal brain ischemia in vivo. Strikingly, deficiency in either protein completely prevented long-term functional motor deficits after cerebral ischemia and strongly reduced brain atrophy as a result of inhibiting phagocytosis of neurons. Correspondingly, in vitro glutamate-stressed neurons reversibly exposed the "*eat-me*" signal phosphatidylserine, leading to their phagocytosis by microglia; this neuronal loss was prevented in the absence of microglia and reduced if microglia were genetically deficient in MerTK or MFG-E8, both of which mediate phosphatidylserine-recognition. Thus, phagocytosis of viable neurons contributes to brain pathology and, surprisingly, blocking this process is strongly beneficial. Therefore, inhibition of specific phagocytic pathways may present therapeutic targets for preventing delayed neuronal loss after transient cerebral ischemia.

phagoptosis | neuroinflammation

Cerebral ischemia is one of the most common causes of death and disability worldwide and occurs as a result of interrupted blood supply to the brain, resulting in neurodegeneration during stroke and vascular dementia. In the ischemic area where the reduction of blood flow is most pronounced (the core), neuronal death follows rapidly as a result of energy depletion. However, in areas of partial ischemia (the penumbra) and in areas around the infarct (peri-infarct), neurons stressed by ischemia or its consequences are lost only after some delay, providing an opportunity for therapeutic interference hours or days after stroke (1, 2).

In addition to the directly neurotoxic effects of ischemia, damage-associated ligands released from dying cells induce a strong inflammatory response, which can cause further neuronal damage. However, inflammation is a self-limiting process and after ischemia and reperfusion, microglia and recruited macrophages clear cell debris and dying cells through phagocytosis (3, 4).

Phagocytosis is generally considered to be a beneficial process that leads to clearance of potentially harmful cellular components and may also contribute to the resolution of inflammation (5). It has been assumed that cells are only phagocytosed after they are committed to die (6); therefore, a potential contribution of phagocytosis to pathology has not been investigated. However, it has recently become clear that viable cells exposed to sublethal stimuli may expose the "*eat-me*" signal phosphatidylserine (PS), leading to their phagocytosis and thus death (7–11).

The recognition of cells exposing PS can be mediated by a variety of proteins and is dependent on the inflammatory state of the macrophage (for review, see ref. 12). For example, two phagocytic proteins that have been shown to be up-regulated by inflammatory activation are: (*i*) Milk fat globule EGF-like factor-8 (MFG-E8), which binds PS on the phagocytic target cell and the vitronectin receptor on macrophages (13); and (*ii*) Mer receptor tyrosine kinase (MerTK), which detects PS-exposing target cells with the help of PS-binding bridging proteins, such as Gas6 and Protein S (14, 15). However, MerTK can also initiate engulfment because of phosphorylation by focal adhesion kinase downstream of the MFG-E8 receptor, the vitronectin receptor (16).

Interestingly, it has been shown that viable neurons in the ischemic penumbra and surrounding brain are labeled by annexin V, indicating PS exposure peaking 3 d after transient ischemia but reversing thereafter (17), and large numbers of stressed neurons and phagocytic microglia are found together in brain regions during and after ischemia (1, 3). We therefore hypothesized that phagocytosis may contribute to delayed neuronal loss after cerebral ischemia. Our data show that phagocytosis executes neuronal death after transient brain ischemia, because blocking phagocytic signaling prevents both the delayed neuronal loss and long-term functional deficits.

Results

MerTK and MFG-E8 Expression Is Up-Regulated After Focal Brain Ischemia. Depending on their inflammatory state, macrophages express and use different phagocytic pathways for the removal of cells exposing *eat-me* signals (for review, see ref. 12). Inflammatory-activated peripheral macrophages have been shown to up-regulate the bridging protein MFG-E8 and the phagocytic receptor MerTK (13, 14, 18), and deficiency in either protein

Significance

Brain ischemia is a major cause of death and disability worldwide, but the cellular mechanisms of delayed neuronal loss and brain atrophy after cerebral ischemia are poorly understood and thus currently untreatable. Surprisingly, we find that after cerebral ischemia, brain macrophages phagocytose viable and functional neurons, causing brain atrophy and motor dysfunction. Our data show that delayed neuronal death and functional impairment after cerebral ischemia can be prevented by blocking specific phagocytic pathways, and therefore highlight new therapeutic targets for stroke and dementia.

Author contributions: J.J.N. and G.C.B. designed research; J.J.N., J.V.E., M.F., and P.K.M. performed research; C.T. contributed new reagents/analytic tools; J.J.N., J.V.E., and M.F. analyzed data; and J.J.N. and G.C.B. wrote the paper.

The authors declare no conflict of interest.

This article is a PNAS Direct Submission.

[1]To whom correspondence may be addressed. E-mail: jonas.neher@uni-tuebingen.de or gcb3@cam.ac.uk.

[2]Present address: Centre for Asthma and Respiratory Disease, Hunter Medical Research Institute, The University of Newcastle, Newcastle, NSW 2305, Australia.

[3]Present address: Glaxo Smith Kline Research and Development, Stevenage SG1 2NY, United Kingdom.

This article contains supporting information online at www.pnas.org/lookup/suppl/doi:10.1073/pnas.1308679110/-/DCSupplemental.

results in pronounced deficits in the removal of cells displaying the *eat-me* signal PS on their surface (14, 19).

With regards to the central nervous system, it has been reported that the brain's macrophages, microglia, express MerTK (15) as well as MFG-E8 (10) in culture. In contrast, MFG-E8 and MerTK show only low expression levels in the naïve brain (20, 21), but are up-regulated in response to inflammatory stimuli (9, 22), in accordance with a partially activated microglial phenotype in vitro (23). Because cerebral ischemia is accompanied by a strong inflammatory response (3), we were interested in learning whether MFG-E8 and MerTK may be up-regulated following brain ischemia. To induce focal ischemia in vivo, the vasoconstrictor endothelin-1 was injected into the striatum of rats or the sensorimotor cortex of mice, following previously published protocols (24–26). These and other studies have shown that endothelin-1 causes a transient, local reduction of blood flow, mimicking the small, local strokes that are common in humans, with a relatively high penumbra/core ratio and delayed inflammation and neuronal loss (27).

Analyzing the infarct region at 1, 3, 7, and 28 d, MerTK staining was only detectable by immunohistochemistry at 3 d after ischemia in rats (Fig. 1*A*), with MFG-E8 levels also being strongly increased at 3 d (Fig. S1). Similar results were obtained after cortical ischemia in mice, where MFG-E8 levels remained increased at 7 d (Fig. 1*B* and Fig. S1). Immunoreactivity for MerTK or MFG-E8 was virtually absent in the contralateral (vehicle-injected) hemisphere (Fig. 1). Thus, these two phagocytic proteins are minimally expressed in the naïve brain, but are strongly and transiently expressed in the infarct at 3–7 d after-ischemia.

Increased protein levels of MerTK and MFG-E8 coincided with activation of microglia/macrophages (hereafter referred to only as microglia), as detected by their affinity for isolectin-B4 (28, 29). MerTK was only detectable in activated microglia, and MFG-E8 was additionally found to opsonize neurons (Fig. 1*B* and Fig. S1), in accordance with its function in bridging microglial receptors and PS-exposing neurons. Furthermore, staining for β-galactosidase expressed under the endogenous milk fat globule-EGF factor 8 (*Mfge8*) promoter in *Mfge8* knockout mice (30) showed protein expression at 3 and 7 d after focal ischemia in both astrocytes and microglia (but not neurons) (Fig. S1), as has been reported during other conditions of brain inflammation (9, 31).

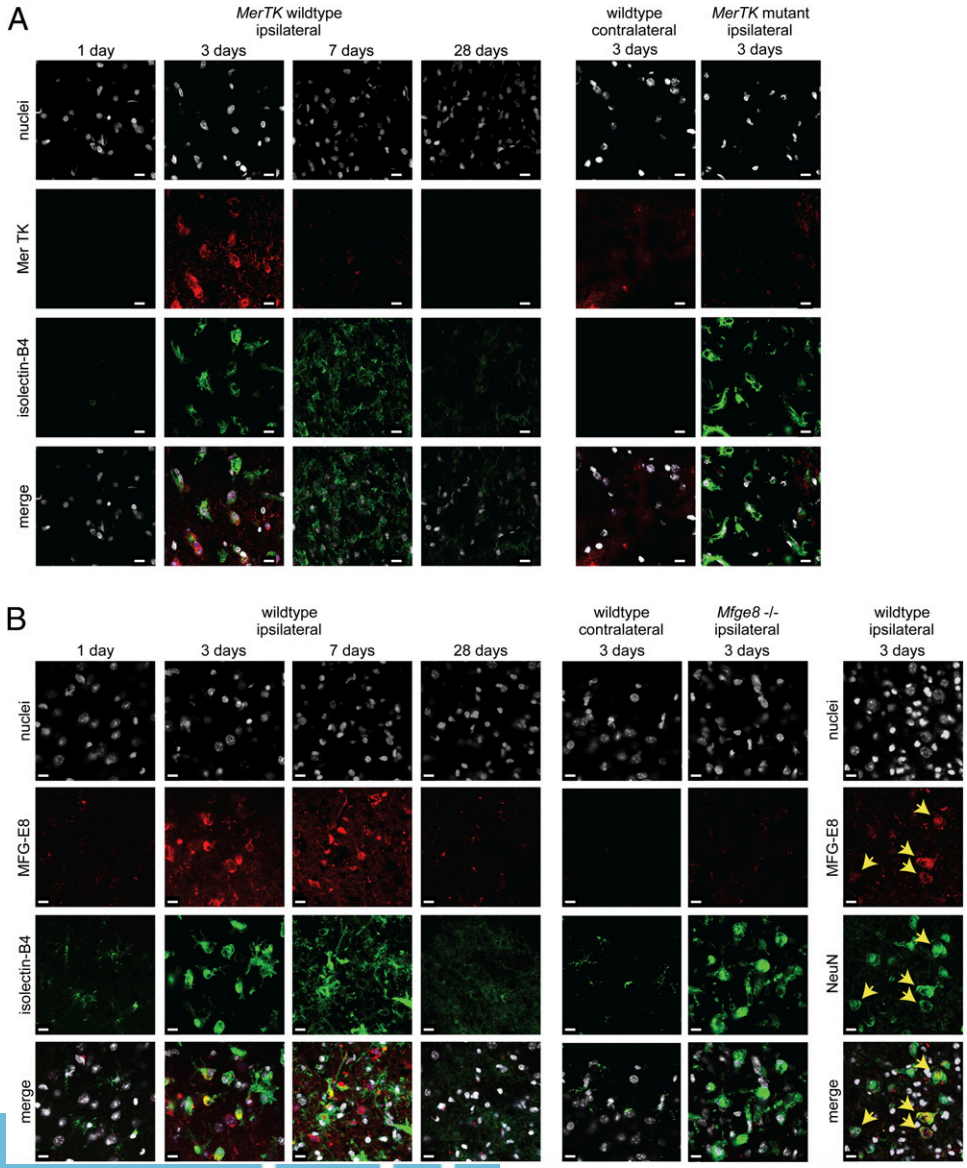

Fig. 1. MerTK and MFG-E8 are transiently up-regulated after focal cerebral ischemia. (*A*) MerTK is highly expressed 3 d after ischemia and colocalizes with activated microglia/macrophages (isolectin-B4; but not astrocytic or neuronal markers). Staining is absent on the contralateral side and in *MerTK* mutant rats, which harbor a deletion of the *MerTK* gene. (*B*) MFG-E8 staining shows protein expression 3 and 7 d after focal cortical ischemia, which is absent on the contralateral side and in *Mfge8* knockout mice. MFG-E8 colocalizes with activated macrophages/microglia (isolectin-B4), but also neurons (NeuN, *Right*, yellow arrows), consistent with its function as a bridging protein. (Scale bars, 10 μm.) Five animals were analyzed per condition.

Of note, MerTK staining was absent in the brains of Royal College of Surgeons rats, which harbor a *MerTK* gene deletion (32), and MFG-E8 staining was absent from *Mfge8* knockout mice (30) subjected to endothelin-1 induced ischemia (Fig. 1), confirming antibody specificity. However, *Mfge8* knockout animals showed pronounced MerTK expression and vice versa (Fig. S1), indicating independent expression of these proteins.

MerTK or MFG-E8 Deficiency Strongly Reduces Motor Deficits After Focal Brain Ischemia. The contribution of MerTK and MFG-E8 to pathology was examined through testing the motor function of animals for 4 wk following striatal or cortical ischemia, respectively. *MerTK* wild-type rats subjected to transient striatal ischemia showed motor deficits in beam-walking (for balance/coordination), ladder-climbing (for grip strength/coordination), and the Montoya staircase (for lateralized skilled forelimb reaching) tasks. These ischemia-induced motor deficits partially recovered over 4 wk, likely because of the well-known adaption, plasticity, and learning effects after ischemic brain damage (33). Strikingly, the motor dysfunction induced by ischemia was strongly decreased in *MerTK* mutant animals compared with wild-type animals (Fig. 2 *A*–*C*). Similarly, after cortical ischemia, *Mfge8* knockout animals showed strongly improved neurological outcome compared with wild-type animals, as measured by beam-walking and ladder-climbing performance (Fig. 2 *D* and *E*). At 4 wk after brain ischemia, the *MerTK*- and *Mfge8*-deficient

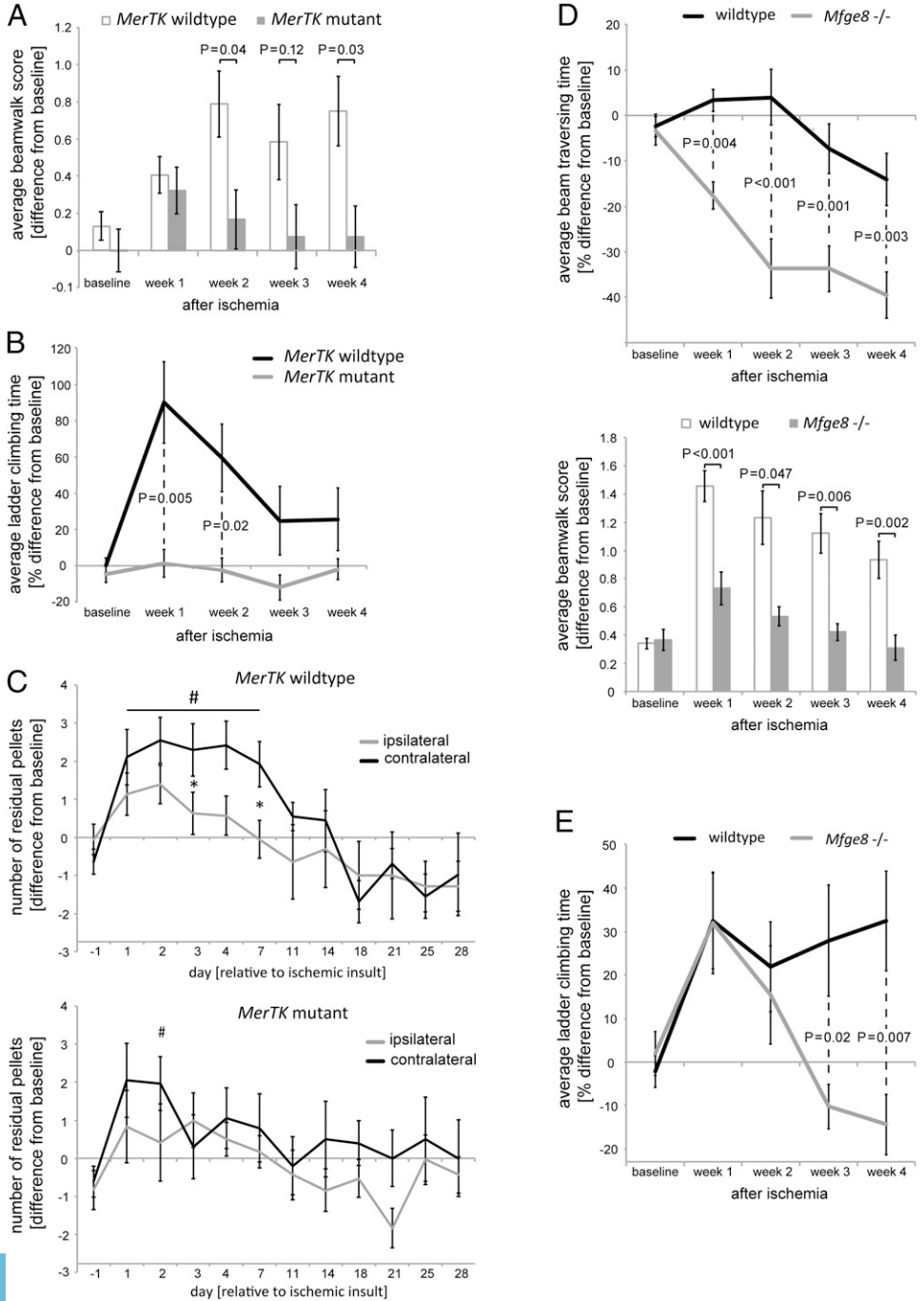

Fig. 2. MerTK- or MFG-E8-deficiency reduces motor deficits after focal cerebral ischemia. (*A*–*C*) *MerTK* mutant rats show (*A*) lower scores for motor impairment when traversing a beam (foot slips were scored as 1, falls from the beam as 2) and (*B*) shorter climbing times of a vertical ladder. (*C*) Only wild-type rats show impairment of the paw contralateral to the infarct in a skilled forepaw-reaching task (*Upper*). The pound sign (#) and asterisk (*) indicate significant differences ($P < 0.05$) compared with baseline and between paws, respectively. (*D*) *Mfge8* knockout mice show more pronounced improvements in their traversing time and less severe motor impairment than wild-type animals when crossing a wooden beam. (*E*) *Mfge8* knockout animals require less time to climb a ladder than wild-type animals. $n \geq 12$ animals per condition.

animals had virtually no remaining motor dysfunctions (Fig. 2), indicating that the lack of MerTK or MFG-E8 provides permanent and substantial protection and benefit.

MerTK Deficiency Reduces Phagocytosis of Neurons and Brain Atrophy After Focal Brain Ischemia. Ischemic stroke leads to a complex series of events that initially involves ischemic neuronal death and brain swelling followed by delayed inflammation, neuronal loss, tissue contraction, and brain atrophy, as well as scar formation (3). To examine these changes in detail, we analyzed neuronal densities and changes in infarct and brain volume at 1, 3, 7, and 28 d after the ischemic insult. Injection of endothelin-1 into the rat striatum resulted in a clearly demarcated infarct (as identified by changes in staining for the neuronal nuclear antigen, NeuN) (Fig. 3*A*) and reproduced essential features of stroke, namely brain swelling at 1 and 3 d after ischemia, microgliosis at 3 and 7 d, brain atrophy starting at 7 d, and scar formation visible at 28 d after ischemia (Fig. 3*A*).

To determine whether the initial ischemic insult and the consequent direct neuronal death were identical in the presence and absence of MerTK, we analyzed infarct volume, brain swelling, and the number of degenerating neurons (Fluorojade C^+) at 1 and 3 d after ischemia. Importantly, it was not possible to distinguish between *MerTK* wild-type and mutant animals on any of these measures (Fig. 3 *B*, *C*, and *E*). Furthermore, cell counts based on the neuronal nuclear antigen, NeuN, showed no loss of neurons at 1 d after ischemia, suggesting that neurons had not yet been phagocytosed. At 3 d, a large proportion of neurons had been lost in the infarct area, but the number of neurons remaining in *MerTK* mutant animals was significantly higher (wild-type: 103 ± 14; *MerTK* mutant: 154 ± 11 neurons per field) (Fig. 3*D*). At the same time, the number of degenerating neurons had significantly decreased and did not differ between genotypes (Fig. 3*E*).

It is known that the initial infarct evolves over time and leads to a decrease in brain volume in both the infarct and surrounding tissue at later time-points (3). Accordingly, at 7 d after ischemia, *MerTK* wild-type animals showed significant loss of brain tissue (Fig. 3*B*, *Right*). In contrast, *MerTK* mutant animals showed no brain atrophy and had significantly smaller infarcts than wild-type animals (Fig. 3*B*). By 28 d, the remaining tissue scar was indistinguishable between genotypes, but the striatal atrophy was decreased by 66 ± 9% in *MerTK* mutant animals compared with wild-type animals (Fig. 3*B*, *Right*), and the atrophy-induced increase in ventricle volume was prevented in *MerTK* mutant rats (Fig. S2). Thus, although the loss of MerTK has no effect on the initial insult and death of neurons, it substantially prevents the delayed loss of live neurons and tissue.

We assessed the innate immune response after ischemia first using isolectin-B4 staining, which labels both phagocytic- and nonphagocytic-activated macrophages/microglia (34). Only few activated microglia were found at 1 d after ischemia, but a strong response was visible in the infarct area at 3 and 7 d, returning almost to baseline by 28 d (Fig. 4*A*). This time-course of microglial recruitment and activation was similar to the time-course of neuronal loss.

At all time-points, the number of activated microglia was the same in *MerTK* mutant and wild-type animals (Fig. 4*A*). In line with an equivalent number of activated microglia being present in *MerTK* wild-type and mutant animals, we could not detect any differences in the inflammatory response as measured by the levels of the inflammatory mediators IL-1β and IL-6, as well as inducible nitric oxide synthase (iNOS) at 3 d postischemia (Fig. S3). These results indicated that the changes in infarct development and brain atrophy were not the result of an altered inflammatory response.

We next assessed the phagocytic activity of microglia in *MerTK* wild-type and mutant animals. A significant proportion of activated microglia had an amoeboid morphology indicative of a phagocytic phenotype (35), and showed large phagolysosomes positive for CD68 (ED1), which is only detectable in phagocytic cells (36). However, at 3 d after ischemia there was a 25 ± 1% reduction in the number of amoeboid microglia (Fig. 4*B*) and a 34 ± 10% reduction in the number of microglia carrying large $CD68^+$ phagolysosomes in the *MerTK* mutant compared with wild-type animals (Fig. S4), indicating that the phagocytic activity was reduced in *MerTK* mutant microglia when the density of neurons was declining most rapidly. No differences were observed at other time-points, in line with the absence of *MerTK* expression at these other time-points (Fig. 1*A*).

Next, the phagocytosis of neurons was directly analyzed at 3 d after ischemia through acquisition of confocal *z*-stacks and 3D image reconstruction to quantify the number of microglia containing neuronal nuclear ($NeuN^+$) material. Strikingly, 51 ± 5% of microglia contained $NeuN^+$ material in wild-type animals, but only 21 ± 2% in MerTK-deficient animals (Fig. 4*C*). Thus, our results indicate that rather than affecting inflammation, MerTK deficiency blocks microglial engulfment of neurons after ischemia. This reaction leads to a pronounced reduction of neuronal loss, and results in strongly reduced brain atrophy and improved motor function in *MerTK* mutant rats.

MFG-E8 Deficiency Reduces Phagocytosis of Neurons and Brain Atrophy After Focal Brain Ischemia. Similar to *MerTK* mutant animals, *Mfge8* knockout mice showed improved functional outcomes after focal ischemia. Analogous to *MerTK* animals, *Mfge8* knockout and wild-type mice showed equivalent infarct size, brain swelling, and numbers of degenerating neurons at 1 and 3 d (Fig. 5 *A*, *B*, and *D*), indicating that the initial insult was independent of genotype and that neurons were not protected from direct neurotoxicity. Although there was no difference in neuronal densities within the infarct between genotypes at any time point (Fig. 5*C*), there was a significant decrease in infarct size at 7 d and almost complete prevention of brain atrophy at 28 d after ischemia in *Mfge8* knockout mice compared with wild-type mice (Fig. 5*B*). This finding indicated that similar to MerTK deficiency, MFG-E8 deficiency also reduced the delayed loss of neurons and brain tissue.

The number of activated microglia was highest at 3 and 7 d after ischemia and did not differ between *Mfge8* knockout and wild-type animals at any time point (Fig. 6*A*). In addition, no differences in the protein levels of the inflammatory mediators IL-1β and IL-6, nor iNOS were detectable at 3 d postischemia (Fig. S3). Furthermore, *Mfge8* deficiency significantly reduced the number of amoeboid microglia by 24 ± 7% at 7 d after ischemia (Fig. 6*B*). Accordingly, *Mfge8* deficiency significantly reduced the number of microglia containing neuronal nuclear material at 3 d after brain ischemia (wild-type 87 ± 7%, *Mfge8* knockout 57 ± 4%) (Fig. 6*C*). These results indicated that *Mfge8* deficiency did not affect the inflammatory response after focal cerebral ischemia, but rather limited microglial phagocytosis of neurons, thereby preventing neuronal loss and brain atrophy and leading to improved motor function.

Neuronal Regeneration Is Limited or Absent After Focal Cerebral Ischemia. To examine whether the differences in neuronal loss/atrophy and functional outcome might be a result of enhanced regenerative capacity in the knockout/mutant strains, recruitment of neuronal precursors was assessed using staining for doublecortin X (DCX). In rats, some DCX^+ cells could be observed in the infarcted striatum (but not the saline-injected contralateral side) at 7 and 28 d after ischemia (Fig. S5). However, recruitment of neuronal precursors was very limited and no differences were observed between *MerTK* wild-type and mutant rats; therefore, it seems unlikely that neuronal replacement made a significant contribution to the improved functional

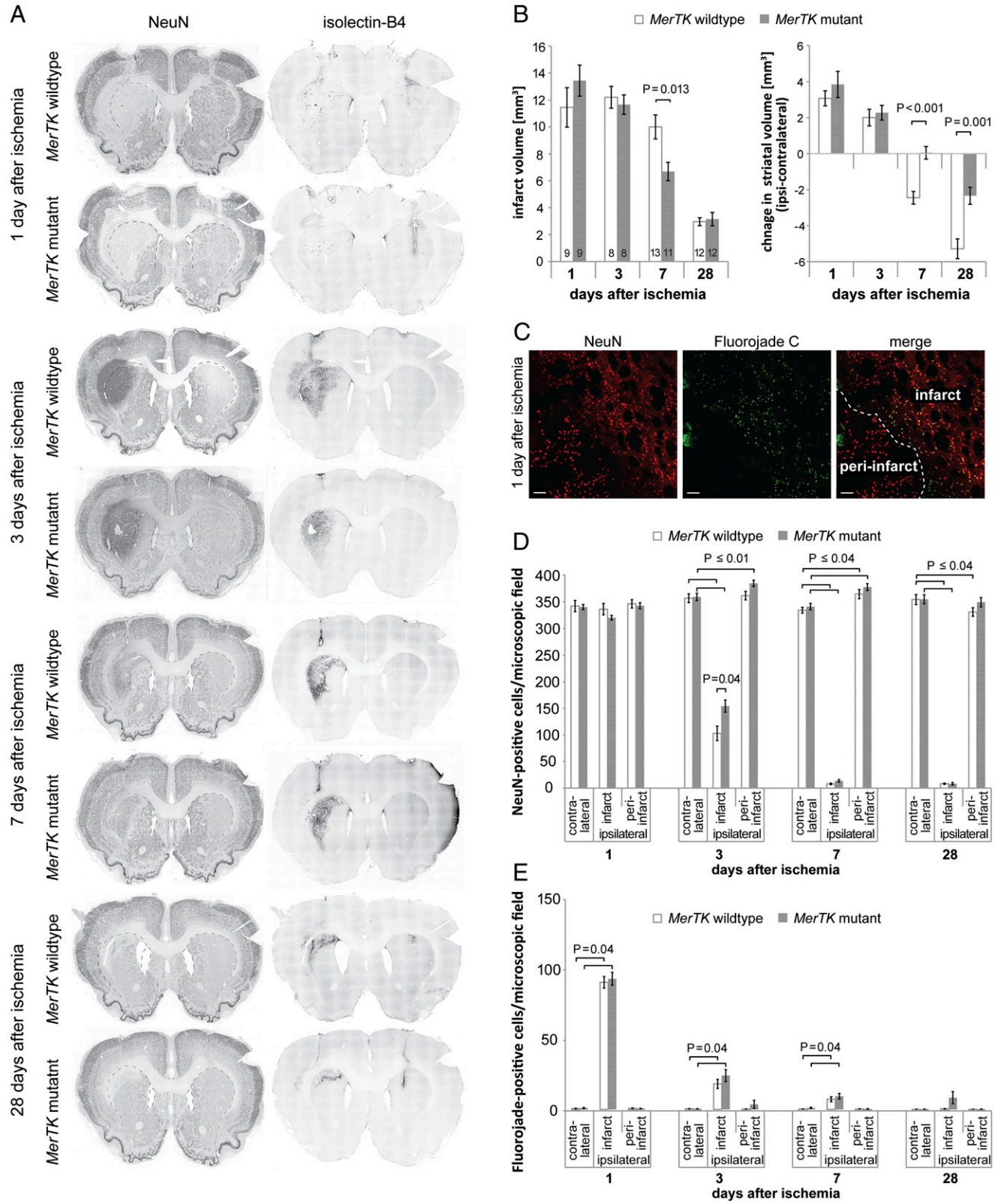

Fig. 3. MerTK deficiency reduces brain atrophy after focal striatal ischemia. (*A*) Macroscopic features of endothelin-1 induced striatal ischemia in *MerTK* wild-type/mutant rats. For comparison, dotted gray lines show the outline of the contralateral (*Right*) striatum in both hemispheres in NeuN-stained sections. Both genotypes show clearly demarcated infarcts, initial brain swelling and strong activation of microglia/macrophages (isolectin-B4). Atrophy is most obvious in wild-type animals at 28 d. (*B*) Quantification of infarct size and changes in striatal volume. Significantly smaller infarct size at 7 d (*Left*) and much reduced striatal atrophy (*Right*) are observed in *MerTK* mutant rats at 7 and 28 d. The number of animals analyzed (*n*) is given at the bottom of each bar. (*C*) Depiction of areas quantified in *D* and *E*. (Scale bars, 20 μm.) (*D*) Quantification of neuronal densities based on the neuronal nuclear marker (NeuN) and (*E*) degenerating neurons (Fluorojade C) (please note that the number of $NeuN^+$ cells includes Fluorojade C^+ cells). $n \geq 5$ per condition. Data presented are means ± SEM.

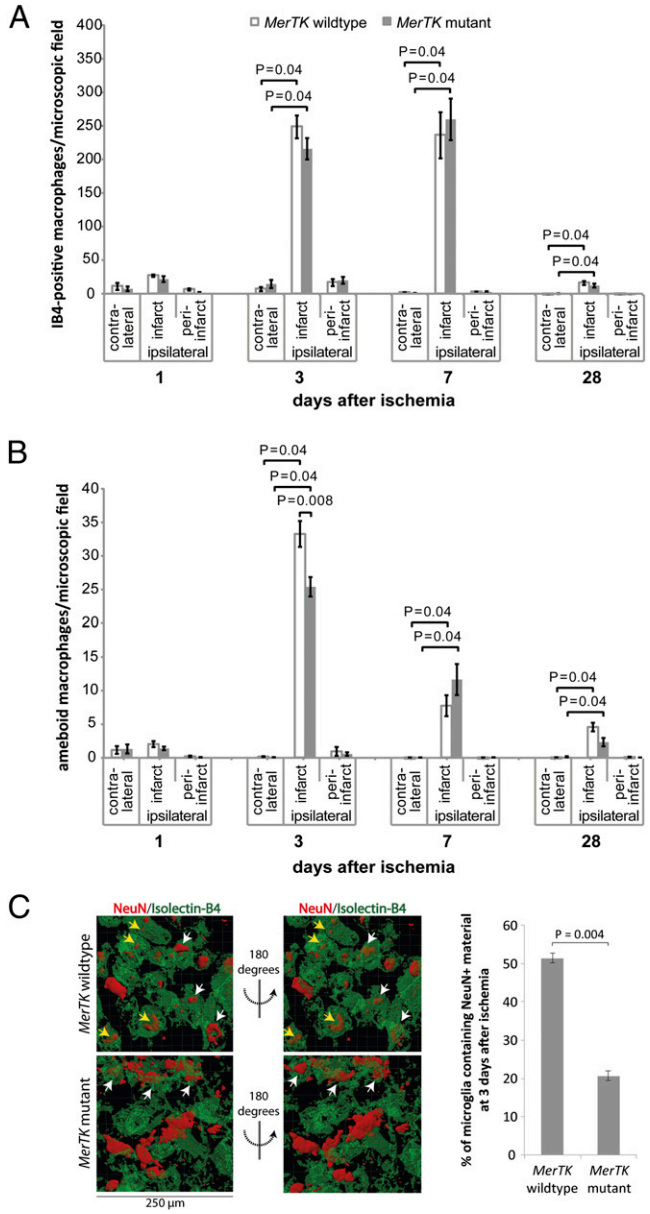

Fig. 4. MerTK deficiency inhibits phagocytosis of neurons after focal striatal ischemia. (*A*) Region-specific densities of activated macrophages/microglia in *MerTK* wild-type and mutant rats. (*B*) Densities of amoeboid macrophages/microglia, indicating phagocytic activity: *MerTK* mutant animals display decreased levels of phagocytic microglia at day 3. (*C*) Quantification of 3D image reconstructions of confocal *z*-stacks of the infarct area. The number of microglia containing neuronal nuclear ($NeuN^+$) material is strongly reduced in *MerTK* mutant animals at 3 d after ischemia ($n \geq 5$ animals per condition). Yellow arrows indicate neurons scored as engulfed; white arrows indicate neurons that are not contained within microglia.

outcome in *MerTK* mutant rats. In accordance with a negligible influence of neuronal regeneration, recruitment of neuronal precursors to the cortex in *Mfge8* knockout and wild-type mice was never observed, even though DCX^+ cells could be clearly seen lining the lateral ventricles (Fig. S5).

Microglial MerTK and MFG-E8 Mediate Loss of Glutamate-Stressed, PS-Exposing Neurons in Vitro. To further test the role of microglial phagocytosis in delayed loss and death of stressed neurons, we also investigated phagocytic signaling in vitro. The release of the excitatory neurotransmitter glutamate causes neuronal stress, activation of microglia and delayed neuronal loss after brain ischemia (1). Within 0.5 h, low glutamate levels (100 µM) caused extensive neuronal exposure of the *eat-me* signal PS, which is known to induce phagocytic uptake via MFG-E8 and MerTK (9–11). Surprisingly, however, 24 h later this PS exposure was fully reversed in the absence of neuronal death or loss (Table 1), indicating transient PS exposure on viable cells. In contrast, high concentrations of glutamate (1 mM) induced irreversible PS exposure (Table 1).

Next, we used a short (6 h) assay to determine: (*i*) if microglia would phagocytose glutamate-stressed, PS-exposing neurons; (*ii*) if phagocytosis was modulated by inflammatory microglial activation; and (*iii*) if this was dependent on MerTK and MFG-E8. Microglia-depleted neuronal/astrocytic cultures were treated with glutamate, the culture medium was exchanged to remove any soluble mediators (possibly including astrocytic MFG-E8), and either naïve microglia or microglia preactivated with a Toll-like receptor 2 (TLR2) agonist were added to the neurons [as TLR2 activation is known to mediate inflammation after brain ischemia (3)]; neuronal loss was assessed 6 h later.

Neuronal death or loss was not affected by the addition of naïve or activated microglia (wild-type, *Mfge8* knockout, or *MerTK* mutant) to untreated neurons (Fig. S6). In the absence of microglia, glutamate caused no significant neuronal loss. However, the addition of microglia to glutamate-treated neurons resulted in significant loss of neurons, which was increased if the microglia were TLR-activated before addition (Table 2). Strikingly, activated microglia from *MerTK* mutant or *Mfge8* knockout animals removed significantly fewer neurons (Table 2), consistent with their role in phagocytosis of stressed neurons. Importantly, delaying the addition of activated wild-type microglia until 24 h after glutamate treatment, when PS-exposure had reversed, also completely prevented neuronal loss (Table 2).

To test whether the inhibition of microglial phagocytosis of stressed neurons in vitro was the result of a change in the microglial inflammatory response in *MerTK* mutant or *Mfge8* knockout microglia, we analyzed inflammatory mediator release. The release of inflammatory mediators (TNF-α, IL-6, or nitric oxide) was equivalent in *MerTK* mutant, *Mfge8* knockout, and wild-type cells (Fig. S6). This finding is in line with our in vivo analysis (Fig. S3).

Having found no differences in the inflammatory response, we next determined if the deficiency in phagocytic uptake of stressed neurons was caused by a general inhibition of phagocytic activity or a specific effect. We have previously shown that the general, PS-independent phagocytic activity of *Mfge8* knockout microglia after TLR activation is equivalent to wild-type cells (9). Similarly, TLR2 or TLR4 agonists enhanced phagocytosis of fluorescent microbeads to the same extent in *MerTK* wild-type and mutant microglia (Fig. S6).

Furthermore, *Mfge8* wild-type and knockout microglia both removed equivalent numbers of dead (propidium iodide-positive) neurons from naïve neuronal cultures incubated with microglia for 6 h (Fig. S6). This result is in line with our previous findings (9) and indicates that the phagocytic defect of *Mfge8* knockout microglia is specific for PS-exposing live neurons but not necrotic neurons, which may be recognized by other signals and opsonins (reviewed in ref. 37). Interestingly, however, we found that dying neurons accumulated in mixed neuronal/glial cultures prepared from *MerTK* mutant animals during the first 7 d in vitro (Fig. S6), indicating deficient phagocytosis of these cells. However, upon TLR-activation, dead cells were efficiently removed (Fig. S6), again highlighting the dependency of phagocytic pathways on the inflammatory status of microglia. Thus, our in vitro results confirm that MerTK and MFG-E8 deficiency have no apparent effect on microglial inflammation or general phagocytic capacity, and that MFG-E8– or MerTK-deficient

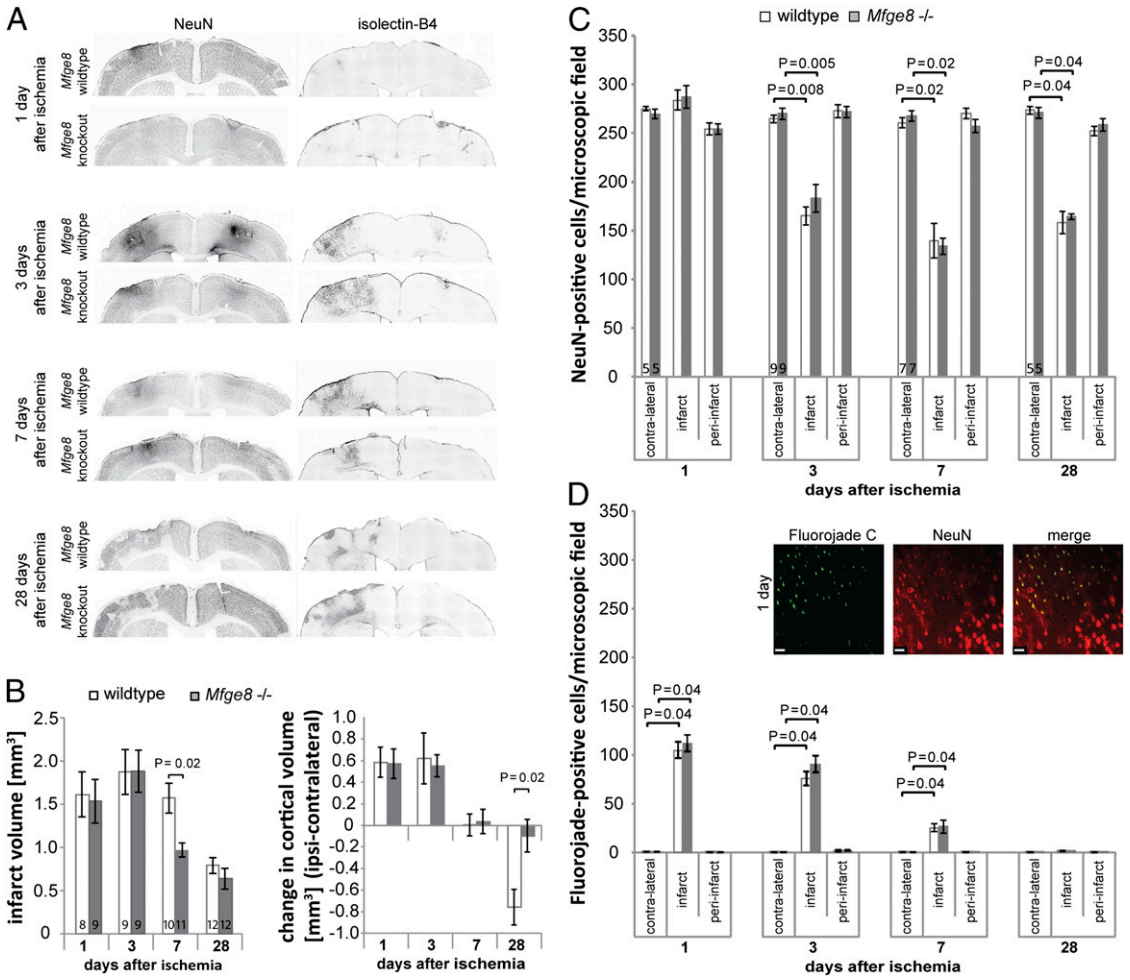

Fig. 5. MFG-E8 deficiency prevents brain atrophy after focal cortical ischemia. (*A*) Macroscopic features of ET-1 induced cortical ischemia in *Mfge8* wild-type/knockout mice. ET-1 injection (left hemisphere) causes cortical infarcts and strong activation of microglia/macrophages (isolectin-B4 staining). (*B*) Quantification of infarct size (*Left*) and cortical volume (*Right*) reveal significantly smaller infarct size at 7 d and virtually complete protection against cortical atrophy at 28 d in *Mfge8* knockout mice. The number of animals analyzed (*n*) is given at the bottom of each bar (*Left*). (*C*) Quantification of neuronal densities based on the neuronal nuclear marker (NeuN) and (*D*) degenerating neurons (Fluorojade C) (please note that the number of NeuN$^+$ cells includes Fluorojade C$^+$ cells). No differences are observed between genotypes. (Scale bars, 20 μm.) $n \geq 5$ animals per condition.

microglia are still capable of removing dead neurons, in line with no accumulation of dead neurons after brain ischemia in vivo (Figs. 3*E* and 5*D*). In contrast, MFG-E8 or MerTK deficiency seems to specifically affect the phagocytosis of stressed but viable neurons during inflammatory conditions.

Discussion

We show herein that a lack of two phagocytic proteins that are required for phagocytosis of PS-exposing cells and are transiently and locally up-regulated after brain ischemia can prevent neuronal loss and death, and as a result improve functional outcome after stroke. Our data point to a mode of neuronal death after brain ischemia that is mediated by phagocytosis of viable cells. This poorly recognized and characterized form of cell death has been called "primary phagocytosis" or "phagoptosis," with the defining characteristic that inhibition of phagocytosis prevents cell death (12, 38). Phagocytosis has previously been assumed to be a beneficial process, but we show here that it can be detrimental and that blocking phagoptosis is functionally beneficial after focal cerebral ischemia.

Phagoptosis has previously been described under physiological conditions, such as macrophage phagocytosis of "aged" erythrocytes and activated neutrophils (39, 40) as well as during development and after subtoxic insults in *Caenorhabditis elegans* (41–43). Additionally, phagoptosis has also been observed after simply inducing PS exposure on the surface of cells (44). Moreover, we have previously characterized phagoptosis of neurons during inflammation induced with TLR ligands in vitro and in vivo (9–11). Therefore, phagocytosis could be a common executioner of cell death and may simply have been overlooked because it leaves no cell corpse to be analyzed.

Exposure of the *eat-me* signal PS has in the past been thought to only occur on dead or dying cells (6, 45). However, it is now clear that many viable cells, including neurons, can expose PS as a result of activation or sublethal stimuli, potentially leading to their phagocytosis and thus death (7–10). We have shown here that glutamate causes PS exposure on otherwise viable neurons in vitro, which can lead to their phagocytosis if activated microglia are present. Furthermore, we have found that neurons after cerebral ischemia in vivo are opsonized with MFG-E8, indicating PS exposure and phagocytic "tagging." Accordingly, others have shown that viable neurons in the postischemic brain are labeled by annexin V, indicating PS exposure that peaks at 3 d after transient ischemia and reverses thereafter (17); these PS-exposed neurons are targets for phagocytosis, as confirmed by our data. Furthermore, we found here that after focal brain

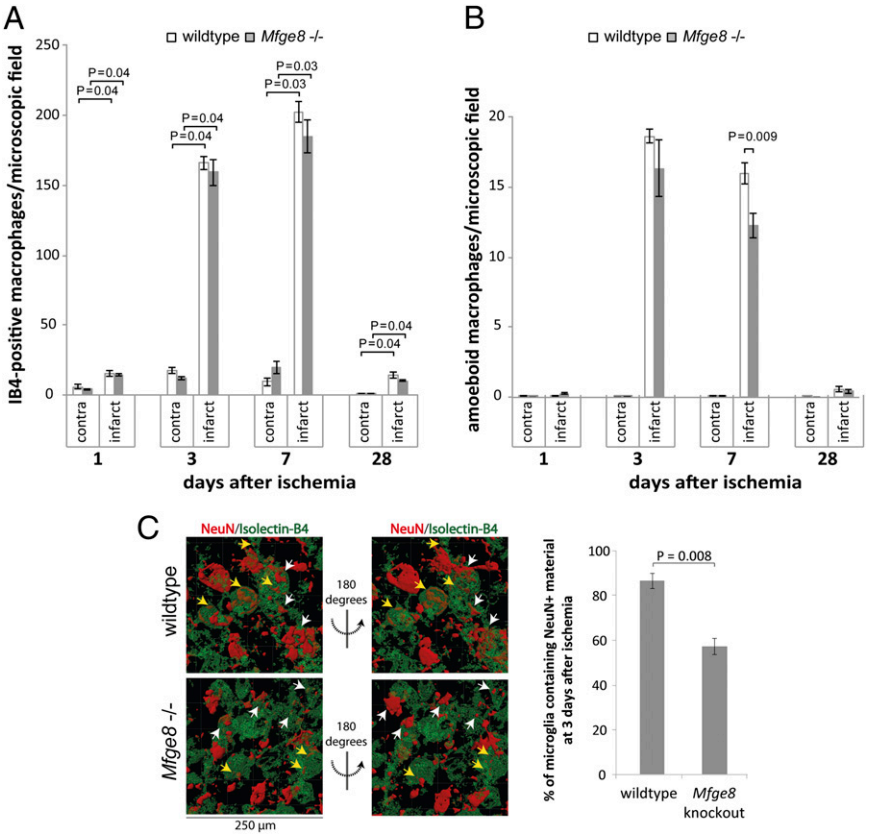

Fig. 6. MFG-E8 deficiency inhibits phagocytosis of neurons after focal cortical ischemia. (*A*) A strong increase in the number of activated macrophages/microglia (isolectin-B4 stained) is observed at 3 and 7 d after ischemia, returns to baseline by 28 d, and does not differ between *Mfge8* wild-type and knockout mice. (*B*) Densities of amoeboid macrophages/microglia, indicating phagocytic activity: *Mfge8* knockout animals display decreased levels of phagocytic cells at day 7. (*C*) Quantification of 3D image reconstructions of confocal *z*-stacks of the infarct area. The number of microglia containing neuronal nuclear ($NeuN^+$) material is significantly reduced in *Mfge8* knockout animals at 3 d after ischemia ($n \geq 5$ animals per condition). Yellow arrows indicate neuronal material scored as engulfed, white arrows indicate neurons that are not contained within microglia.

ischemia, activated macrophages/microglia in the infarct area showed delayed and transient up-regulation of MerTK and MFG-E8, both of which are known to facilitate recognition of PS. PS can be reversibly exposed on stressed but viable cells (7–10) and, in accordance with phagocytosis of viable neurons, deficiency in MerTK or MFG-E8 protected neurons from phagocytic uptake after glutamate treatment in vitro and led to strongly reduced loss of brain tissue after transient cerebral ischemia in vivo.

MerTK can activate actin rearrangement and engulfment either as a result of: (*i*) engagement by bridging molecules for PS recognition (e.g., Gas6, Protein S), or (*ii*) phosphorylation by focal adhesion kinase downstream of the MFG-E8 receptor, the vitronectin receptor (16). Thus, the protective effect in *MerTK* mutant animals could result from the prevention of PS-induced phagocytosis mediated by both MFG-E8 and other adaptor proteins.

MerTK or MFG-E8 deficiency protected the postischemic brain by preventing delayed loss of viable brain tissue, rather than reducing the size of the residual infarct. This delayed loss of viable tissue after ischemia (that is prevented by blocking phagocytosis) must either occur in the infarct itself or in peri-infarct areas. In the former case, areas at the edge of the infarct (the penumbra) may revert to healthy tissue when phagocytosis is blocked; in the latter case, brain areas around the infarct normally atrophy, but this may be prevented when phagocytosis is blocked. Importantly, the delayed atrophy of areas around the infarct has been described in human stroke (46, 47) and animal models of stroke (2).

Of note, microglial deficiency in MerTK or MFG-E8 did not lead to the accumulation of dying neurons in vivo and we found that *Mfge8* knockout microglia were still able to remove dead cells when incubated with neurons for 6 h (Fig. S6). MFG-E8 has been reported to mediate microglial phagocytosis of apoptotic neuroblastoma cells (20), but this has not been confirmed as yet for primary neurons. Interestingly, *MerTK* mutant microglia displayed reduced phagocytic removal of dead cells in naïve cultures, but when activated with a TLR-agonist, phagocytosis of dead cells was enabled. Correspondingly, after brain ischemia in vivo there was no increase in degenerating neurons in knockout/mutant animals (as measured by Fluorojade C staining), indicating that phagocytosis of dead neurons was not impaired, possibly because of additional *eat-me* signals being displayed or released by dead cells (37). Importantly, the lack of accumulation of dead or dying cells despite inhibition of phagocytosis indicates that the cells protected from phagocytosis must have been alive when they were eaten. Although it is possible that Fluorojade C staining does not label all dead and dying neurons, the protective effect against brain atrophy and the long-lasting improved functional outcome provide strong evidence that live cells, but not dying cells, were preserved in *MerTK* mutant/*Mfge8* knockout animals.

Phagocytic engulfment of PS-exposing cells can suppress proinflammatory signaling and lead to the induction of an anti-inflammatory phenotype in the engulfing cell (for review, see ref. 48). In line with this observation, knockout of MFG-E8 or MerTK can lead to enhanced inflammation (see, for example,

Table 1. Glutamate-stressed neurons reversibly expose phosphatidylserine

	% Annexin V^+ neurons	
Treatment	100 µM glutamate	1 mM glutamate
Untreated	7 ± 2%	
0.5 h after glutamate	53 ± 4%*	77 ± 9%*
24 h after glutamate	6 ± 2%	73 ± 4%

*$P < 0.01$ vs. untreated control.

Table 2. Microglial MerTK and MFG-E8 mediate loss of glutamate-stressed but viable neurons in vitro

Time of glutamate treatment	Microglial status	Microglial genotype	Change in neuronal population after adding microglia for 6 h*
+ microglia after 0.5 h 100 μM glutamate	No microglia		−2 ± 3%
	Naïve	Wild-type	−22 ± 3%†
	TLR-activated	*MerTK* wild-type	−36 ± 16%
		MerTK mutant	−5 ± 10%‡
		Mfge8 wild-type	−49 ± 5%§
		Mfge8 knockout	−32 ± 6%¶
+ microglia after 24 h 100 μM glutamate	No microglia		−2 ± 2%
	TLR-activated	Wild-type	−8 ± 3% ‖

*No significant differences were observed between groups for untreated neurons.
†$P < 0.01$ vs. no microglia.
‡$P < 0.05$ vs. TLR-activated *MerTK* wild-type microglia.
§$P < 0.05$ vs. naïve wild-type microglia.
¶$P < 0.05$ vs. TLR-activated *Mfge8* wild-type microglia.
‖$P < 0.05$ vs. TLR-activated wild-type microglia, 0.5 h glutamate.

refs. 15 and 49). Of note, two studies investigating models of permanent cerebral ischemia have reported protective effects mediated by MFG-E8 through modulation of the inflammatory response. One study reported enhanced IL-1β production and larger infarcts in *Mfge8* knockout mice (50), whereas the other correspondingly reported suppression of inflammation after intravenous treatment with recombinant MFG-E8 and reduced infarct size (51). In contrast, we could not detect any significant changes in the inflammatory response after focal cerebral ischemia as measured by the number of activated microglia, as well as the release of inflammatory mediators both in vitro and in vivo (Figs. S3 and S6). This difference may be explained by the use of a model of permanent brain ischemia in the aforementioned studies, which produces a much more severe insult, leading to a large core region with direct neurotoxicity and a small penumbra area, as well as a severe inflammatory response resulting from disintegration of necrotic cells. It is therefore likely that any protection resulting from inhibition of phagoptosis would have been small relative to the total infarct size, and that the inflammatory response would have been much stronger than we observed here, thereby potentially explaining the difference in our results.

Our data indicates that phagocytosis of neurons does not occur until at least 24 h after focal cerebral ischemia and that MerTK and MFG-E8 expression is transient and restricted to the infarct area. Therefore, MerTK- and MFG-E8–mediated phagocytosis could be an interesting therapeutic target for stroke and related pathologies, particularly because disruption of the blood-brain barrier as a result of cerebral ischemia may allow entry of drugs into the infarct area. As stroke remains one of the most common causes of disability and death in the world (52), treatments aimed at preventing phagocytosis-induced neuronal death should be investigated.

Methods and Materials

All experiments were performed in accordance with the UK Animals (Scientific Procedures) Act (1986) and approved by the Cambridge University local ethical committee.

Animals. All animals were bred and housed locally. Wild-type C57BL/6 and homozygous *Mfge8* knockout mice were used (30). Homozygous Royal College of Surgeons rats, which have a spontaneous deletion of the *MerTK* gene (32), and a control wild-type strain were generously provided by John Greenwood, Institute of Ophthalmology, University College London, London.

Cell Culture Experiments. Primary cerebellar neuronal/astrocytic/microglial and pure microglial cultures were prepared as described previously (53). Selective elimination of microglia using L-leucine-methyl-ester, phagocytosis assays, cell counts, annexin V staining, and assessment of phagocytic capacity were performed as previously described (10). Of note, before adding microglia to glutamate-treated neurons, the culture medium was exchanged with medium from wild-type sister cultures.

Surgical Procedure. Ten-week-old male *MerTK* wild-type/mutant or *Mfge8* wild-type/knockout mice received bilateral stereotactic injections of endothelin-1 (ET-1) and vehicle under anesthesia and analgesia. Stereotactic coordinates were [relative to bregma according to Paxinos and Watson (1982) and Paxinos and Franklin (2001)]: rat striatum: AP +1.2 mm, ML ± 3 mm, DV −5 mm; mouse sensorimotor cortex: AP +0.6 mm, ML ± 2.2 mm, DV −1.7 mm, similar to published protocols (24–26). ET-1 (Bachem) was infused over 5/10 min in rats/mice at 50/300 pmoles in 2/1 μL, respectively. Animals were deeply anesthetized and transcardially perfused with cold PBS followed by 4% (wt/vol) paraformaldehyde. Cryoprotected brains were cut into 40-μm-thick (rats) or 25-μm-thick (mice) coronal sections and immunohistochemistry was performed as previously described (9).

Quantification of Infarct Size, Brain Volume, Cellular Densities, and Phagocytosis in Vivo. Every fifth and fourth section containing the infarct was analyzed for rats and mice, respectively. Stained sections were scanned using a Leica DMI6000 microscope and infarct size was measured using Image J software for each section based on changes in staining for neuronal nuclei (NeuN), or alternatively Fluorojade C (early time-points) or isolectin-B4 (later time-points), yielding equivalent results. Areas covered by the striatum and overlying cortex in rats and the cortex in mice were measured based on anatomical landmarks according to Paxinos and Watson (1982) and Paxinos and Franklin (2001) in 15–18 sections per rat and 9–12 sections per mouse, covering the infarct area and at least two additional rostral and caudal sections. Volumes were calculated by multiplying the sum of the areas of all sections by the distance between analyzed slices (34).

To analyze phagocytic uptake of neurons, confocal *z*-stacks of the infarct area were taken with a 63× objective and 3D reconstructions were generated using Imaris 7.4.0 software (with fixed thresholds for reconstructions). More than 600 individual microglia from five animals per group were analyzed to determine differences in uptake of neuronal nuclear ($NeuN^+$) material.

Analysis of Inflammatory Mediators in Vivo. To analyze the protein levels of iNOS, IL-1β and IL-6, proteins were isolated from brain sections using Qproteome FFPE Tissue Kit (Qiagen) according to the manufacturer's protocol (the two hemispheres were separated and four hemispheres from anatomically matched sections containing the infarct were pooled). Protein content of samples was quantified with bicinchoninic acid assay (Pierce Biotechnology) and 15 μg of protein were loaded for each sample. Proteins were analyzed by standard SDS PAGE and Western blotting. Proteins were detected using mouse anti-mouse iNOS (BD Transduction Laboratories; 1:250), rabbit anti-IL-1β (Santa Cruz, sc-7884; 1:1,000), mouse anti-IL6 (Abcam, ab-9324: 1:250), and mouse anti- GAPDH (HyTest; 1:50,000) antibodies and appropriate secondary antibodies conjugated with horse-radish peroxidase. Luminescence signal was recorded using a XS Stella 3200 device (Raytest) and protein band intensity was then quantified using AIDA Image Analyzer software, ensuring that quantified bands were not overexposed. Signal intensities were normalized for GAPDH intensities.

Behavioral Testing. Forelimb and hindlimb impairments were evaluated using the beam-walking test, which sensitively detects sensorimotor deficits following cerebral ischemia in rats and mice (54, 55). Climbing tests were used to assess grip strength and general sensorimotor impairment (56). The Montoya staircase was used as a measure of lateralized skilled forelimb motor function in rats (57).

Statistical Analysis. Statistical analysis was performed using SPSS software and nonparametric tests throughout. Kruskal–Wallis and Friedman tests were used to analyze differences between more than two independent and dependent samples, respectively; Mann–Whitney and Wilcoxon tests were used for pairwise comparison of independent and related samples, respectively. Results were considered to be statistically significant if $P < 0.05$. All data are presented as means ± SEM. The number of independent repeats (n) for each experiment is specified in the figure legends.

ACKNOWLEDGMENTS. We thank Dr. Aviva M. Tolkovsky for insightful discussion and advice. This work was funded by the Wellcome Trust, United Kingdom, Grant RG50995, and a Roman Herzog Postdoctoral Fellowship of the Hertie Foundation (Frankfurt, Germany) (to J.J.N.).

1. Lo EH (2008) A new penumbra: Transitioning from injury into repair after stroke. *Nat Med* 14(5):497–500.
2. Karl JM, Alaverdashvili M, Cross AR, Whishaw IQ (2010) Thinning, movement, and volume loss of residual cortical tissue occurs after stroke in the adult rat as identified by histological and magnetic resonance imaging analysis. *Neuroscience* 170(1):123–137.
3. Iadecola C, Anrather J (2011) The immunology of stroke: From mechanisms to translation. *Nat Med* 17(7):796–808.
4. Ransohoff RM, Brown MA (2012) Innate immunity in the central nervous system. *J Clin Invest* 122(4):1164–1171.
5. Neumann H, Kotter MR, Franklin RJ (2009) Debris clearance by microglia: An essential link between degeneration and regeneration. *Brain* 132(Pt 2):288–295.
6. Ravichandran KS (2003) "Recruitment signals" from apoptotic cells: Invitation to a quiet meal. *Cell* 113(7):817–820.
7. Jitkaew S, Witasp E, Zhang S, Kagan VE, Fadeel B (2009) Induction of caspase- and reactive oxygen species-independent phosphatidylserine externalization in primary human neutrophils: Role in macrophage recognition and engulfment. *J Leukoc Biol* 85(3):427–437.
8. Tyurina YY, et al. (2007) Nitrosative stress inhibits the aminophospholipid translocase resulting in phosphatidylserine externalization and macrophage engulfment: Implications for the resolution of inflammation. *J Biol Chem* 282(11):8498–8509.
9. Fricker M, et al. (2012) MFG-E8 mediates primary phagocytosis of viable neurons during neuroinflammation. *J Neurosci* 32(8):2657–2666.
10. Neher JJ, et al. (2011) Inhibition of microglial phagocytosis is sufficient to prevent inflammatory neuronal death. *J Immunol* 186(8):4973–4983.
11. Neniskyte U, Neher JJ, Brown GC (2011) Neuronal death induced by nanomolar amyloid β is mediated by primary phagocytosis of neurons by microglia. *J Biol Chem* 286(46):39904–39913.
12. Neher JJ, Neniskyte U, Brown GC (2012) Primary phagocytosis of neurons by inflamed microglia: Potential roles in neurodegeneration. *Front Pharmacol* 3:27.
13. Hanayama R, et al. (2002) Identification of a factor that links apoptotic cells to phagocytes. *Nature* 417(6885):182–187.
14. Scott RS, et al. (2001) Phagocytosis and clearance of apoptotic cells is mediated by MER. *Nature* 411(6834):207–211.
15. Grommes C, et al. (2008) Regulation of microglial phagocytosis and inflammatory gene expression by Gas6 acting on the Axl/Mer family of tyrosine kinases. *J Neuroimmune Pharmacol* 3(2):130–140.
16. Wu Y, Singh S, Georgescu MM, Birge RB (2005) A role for Mer tyrosine kinase in alphavbeta5 integrin-mediated phagocytosis of apoptotic cells. *J Cell Sci* 118(Pt 3):539–553.
17. Mari C, et al. (2004) Detection of focal hypoxic-ischemic injury and neuronal stress in a rodent model of unilateral MCA occlusion/reperfusion using radiolabeled annexin V. *Eur J Nucl Med Mol Imaging* 31(5):733–739.
18. Shao WH, Zhen Y, Eisenberg RA, Cohen PL (2009) The Mer receptor tyrosine kinase is expressed on discrete macrophage subpopulations and mainly uses Gas6 as its ligand for uptake of apoptotic cells. *Clin Immunol* 133(1):138–144.
19. Hanayama R, et al. (2004) Autoimmune disease and impaired uptake of apoptotic cells in MFG-E8-deficient mice. *Science* 304(5674):1147–1150.
20. Fuller AD, Van Eldik LJ (2008) MFG-E8 regulates microglial phagocytosis of apoptotic neurons. *J Neuroimmune Pharmacol* 3(4):246–256.
21. Gautier EL, et al.; Immunological Genome Consortium (2012) Gene-expression profiles and transcriptional regulatory pathways that underlie the identity and diversity of mouse tissue macrophages. *Nat Immunol* 13(11):1118–1128.
22. Binder MD, et al. (2008) Gas6 deficiency increases oligodendrocyte loss and microglial activation in response to cuprizone-induced demyelination. *J Neurosci* 28(20):5195–5206.
23. Ransohoff RM, Perry VH (2009) Microglial physiology: Unique stimuli, specialized responses. *Annu Rev Immunol* 27:119–145.
24. Hughes PM, et al. (2003) Focal lesions in the rat central nervous system induced by endothelin-1. *J Neuropathol Exp Neurol* 62(12):1276–1286.
25. Fuxe K, et al. (1992) Involvement of local ischemia in endothelin-1 induced lesions of the neostriatum of the anaesthetized rat. *Exp Brain Res* 88(1):131–139.
26. Wang Y, Jin K, Greenberg DA (2007) Neurogenesis associated with endothelin-induced cortical infarction in the mouse. *Brain Res* 1167:118–122.
27. Durukan A, Tatlisumak T (2007) Acute ischemic stroke: Overview of major experimental rodent models, pathophysiology, and therapy of focal cerebral ischemia. *Pharmacol Biochem Behav* 87(1):179–197.
28. Maddox DE, Shibata S, Goldstein IJ (1982) Stimulated macrophages express a new glycoprotein receptor reactive with *Griffonia simplicifolia* I-B4 isolectin. *Proc Natl Acad Sci USA* 79(1):166–170.
29. Zhang Z, Chopp M, Powers C (1997) Temporal profile of microglial response following transient (2 h) middle cerebral artery occlusion. *Brain Res* 744(2):189–198.
30. Silvestre JS, et al. (2005) Lactadherin promotes VEGF-dependent neovascularization. *Nat Med* 11(5):499–506.
31. Boddaert J, et al. (2007) Evidence of a role for lactadherin in Alzheimer's disease. *Am J Pathol* 170(3):921–929.
32. D'Cruz PM, et al. (2000) Mutation of the receptor tyrosine kinase gene Mertk in the retinal dystrophic RCS rat. *Hum Mol Genet* 9(4):645–651.
33. Moskowitz MA, Lo EH, Iadecola C (2010) The science of stroke: Mechanisms in search of treatments. *Neuron* 67(2):181–198.
34. Buchan AM, Slivka A, Xue D (1992) The effect of the NMDA receptor antagonist MK-801 on cerebral blood flow and infarct volume in experimental focal stroke. *Brain Res* 574(1-2):171–177.
35. Bohatschek M, Kloss CU, Kalla R, Raivich G (2001) In vitro model of microglial deramification: Ramified microglia transform into amoeboid phagocytes following addition of brain cell membranes to microglia-astrocyte cocultures. *J Neurosci Res* 64(5):508–522.
36. Graeber MB, Streit WJ (2010) Microglia: Biology and pathology. *Acta Neuropathol* 119(1):89–105.
37. Poon IK, Hulett MD, Parish CR (2010) Molecular mechanisms of late apoptotic/necrotic cell clearance. *Cell Death Differ* 17(3):381–397.
38. Brown GC, Neher JJ (2012) Eaten alive! Cell death by primary phagocytosis: 'Phagoptosis'. *Trends Biochem Sci* 37(8):325–332.
39. Lee SJ, Park SY, Jung MY, Bae SM, Kim IS (2011) Mechanism for phosphatidylserine-dependent erythrophagocytosis in mouse liver. *Blood* 117(19):5215–5223.
40. Lagasse E, Weissman IL (1994) bcl-2 inhibits apoptosis of neutrophils but not their engulfment by macrophages. *J Exp Med* 179(3):1047–1052.
41. Reddien PW, Cameron S, Horvitz HR (2001) Phagocytosis promotes programmed cell death in *C. elegans*. *Nature* 412(6843):198–202.
42. Hoeppner DJ, Hengartner MO, Schnabel R (2001) Engulfment genes cooperate with ced-3 to promote cell death in *Caenorhabditis elegans*. *Nature* 412(6843):202–206.
43. Neukomm LJ, et al. (2011) Loss of the RhoGAP SRGP-1 promotes the clearance of dead and injured cells in *Caenorhabditis elegans*. *Nat Cell Biol* 13(1):79–86.
44. Darland-Ransom M, et al. (2008) Role of *C. elegans* TAT-1 protein in maintaining plasma membrane phosphatidylserine asymmetry. *Science* 320(5875):528–531.
45. Savill J, Gregory C (2007) Apoptotic PS to phagocyte TIM-4: Eat me. *Immunity* 27(6):830–832.
46. Kraemer M, et al. (2004) Delayed shrinkage of the brain after ischemic stroke: Preliminary observations with voxel-guided morphometry. *J Neuroimaging* 14(3):265–272.
47. Gauthier LV, Taub E, Mark VW, Barghi A, Uswatte G (2012) Atrophy of spared gray matter tissue predicts poorer motor recovery and rehabilitation response in chronic stroke. *Stroke* 43(2):453–457.
48. Wu Y, Tibrewal N, Birge RB (2006) Phosphatidylserine recognition by phagocytes: A view to a kill. *Trends Cell Biol* 16(4):189–197.
49. Eken C, et al. (2010) Ectosomes released by polymorphonuclear neutrophils induce a MerTK-dependent anti-inflammatory pathway in macrophages. *J Biol Chem* 285(51):39914–39921.
50. Deroide N, et al. (2013) MFGE8 inhibits inflammasome-induced IL-1β production and limits postischemic cerebral injury. *J Clin Invest* 123(3):1176–1181.
51. Cheyuo C, et al. (2012) Recombinant human MFG-E8 attenuates cerebral ischemic injury: Its role in anti-inflammation and anti-apoptosis. *Neuropharmacology* 62(2):890–900.
52. Macrez R, et al. (2011) Stroke and the immune system: From pathophysiology to new therapeutic strategies. *Lancet Neurol* 10(5):471–480.
53. Neher JJ, Brown GC, Kinsner-Ovaskainen A, Bal-Price A (2010) Inflammation and reactive oxygen/nitrogen species in glial/neuronal cultures. *Neuromethods* 56:331–347.
54. Gupta R, Singh M, Sharma A (2003) Neuroprotective effect of antioxidants on ischaemia and reperfusion-induced cerebral injury. *Pharmacol Res* 48(2):209–215.
55. Adén U, et al. (2002) MRI evaluation and functional assessment of brain injury after hypoxic ischemia in neonatal mice. *Stroke* 33(5):1405–1410.
56. Boltze J, et al. (2006) The stairway: A novel behavioral test detecting sensomotoric stroke deficits in rats. *Artif Organs* 30(10):756–763.
57. Montoya CP, Campbell-Hope LJ, Pemberton KD, Dunnett SB (1991) The "staircase test": A measure of independent forelimb reaching and grasping abilities in rats. *J Neurosci Methods* 36(2–3):219–228.